Electronic Supplementary Material (ESI) for Journal of Materials Chemistry A.

Electronic Supplementary Information for

Dual-sized NiFe layered double hydroxides *in-situ* grown on oxygen-decorated self-dispersal nanocarbon as enhanced water oxidation catalysts

Xiaolin Zhu,[a,b,†] *Cheng Tang,*[a,†] *Hao-Fan Wang,*[a] *Qiang Zhang,*[a,*] *Chaohe Yang,*[b] *and Fei Wei*[a]

[a] Beijing Key Laboratory of Green Chemical Reaction Engineering and Technology, Department of Chemical Engineering, Tsinghua University, Beijing 100084, China

[b] State Key Laboratory of Heavy Oil Processing, China University of Petroleum, Qingdao 266580, China

[*] Correspondence concerning this article should be addressed to Q. Zhang
Email: zhang-qiang@mails.tsinghua.edu.cn

[†] X. Zhu and C. Tang contribute equally.

1. Supplementary Figures

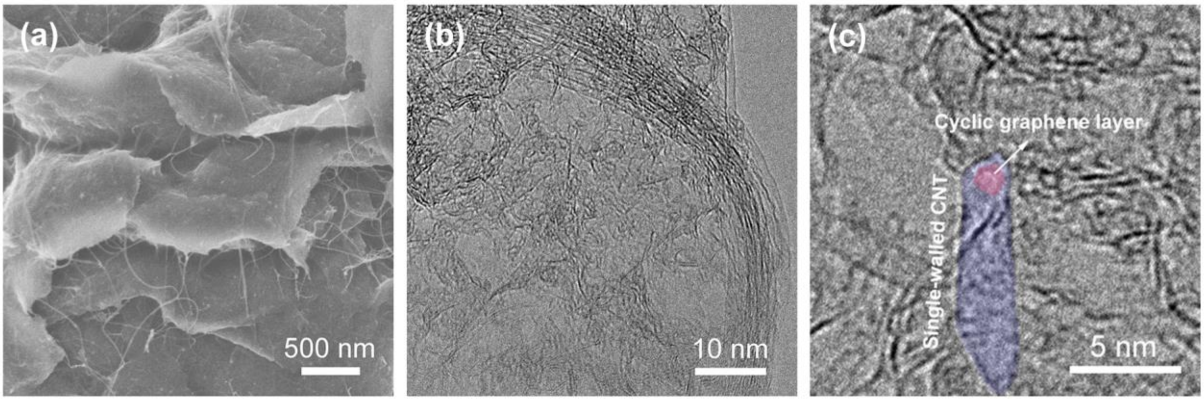

Fig. S1 Morphology of the graphene/single-walled CNT hybrids mass produced in a fluidized bed reactor. (a) SEM image showing that the single-walled CNTs are anchored on and sandwiched between the graphene sheets; (b) TEM and (c) high resolution TEM images illustrating the interface between CNTs and graphene layer.

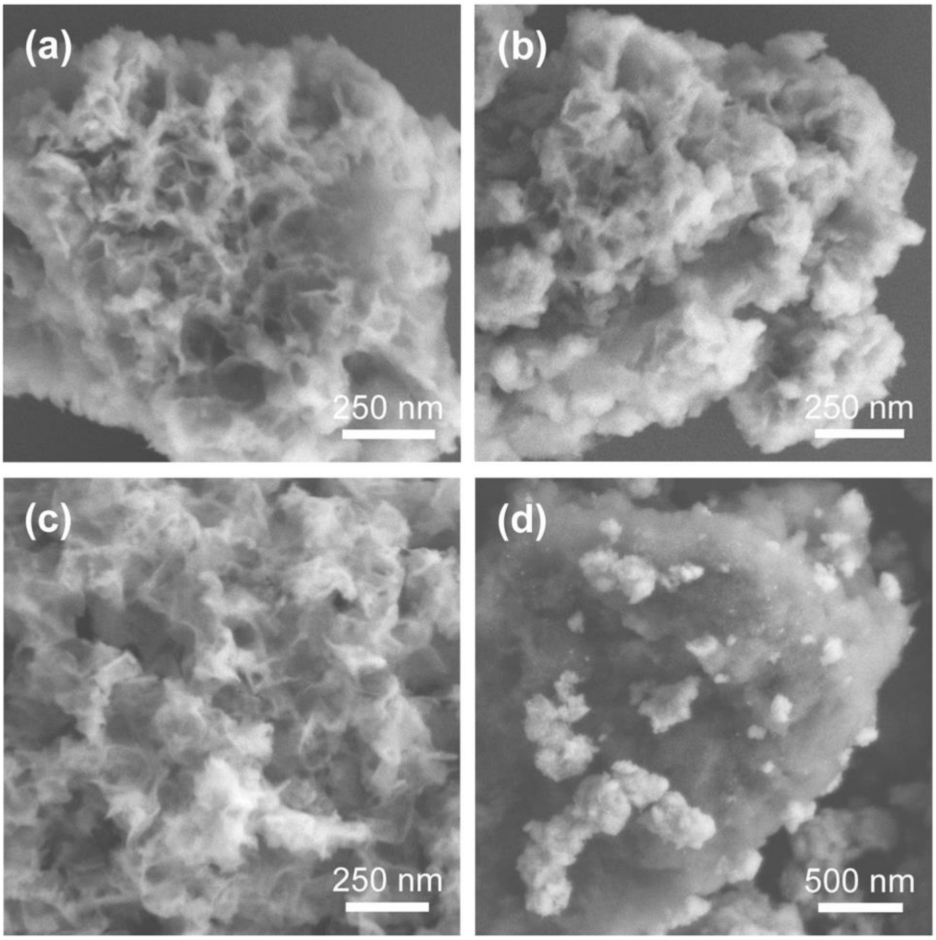

Fig. S2 SEM images of the (a) LDH/oGSH, (b) LDH/GSH, (c) bulk LDH, and (d) LDH+oGSH samples. The oxygen-containing functional groups decorated on oGSH adsorbed and anchored the NiFe LDH precursors onto the topology defects for in-situ nucleation, thereby resulting in a more uniform dispersion of the as-grown LDH plates compared with the LDH/GSH and LDH+oGSH control samples.

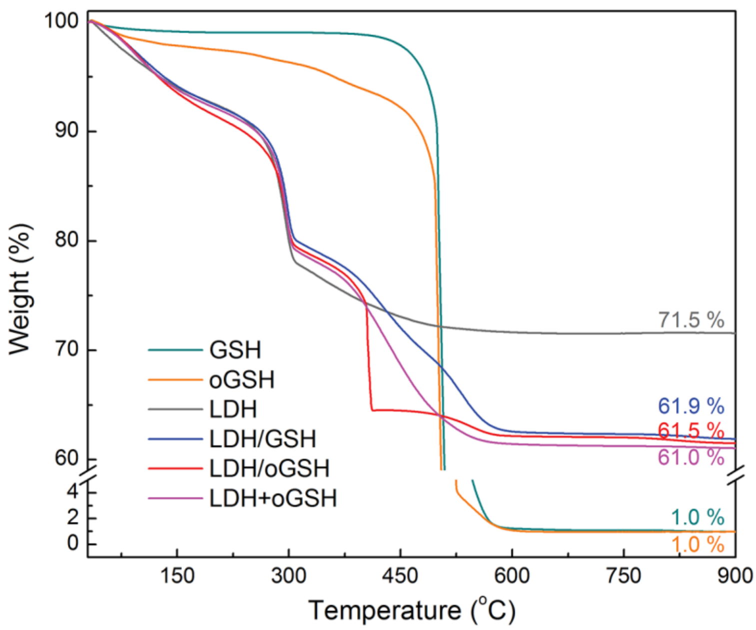

Fig. S3 TGA curves of LDH/oGSH and control samples. Based on the reasonable assumption that the weight loss ratio of LDH was consistent in bulk LDH and relevant complexes, the mass fractions of nanocarbon materials in LDH/GSH, LDH/oGSH, and LDH+oGSH samples were determined to be 13.7, 14.3, and 14.9 wt.%, respectively.

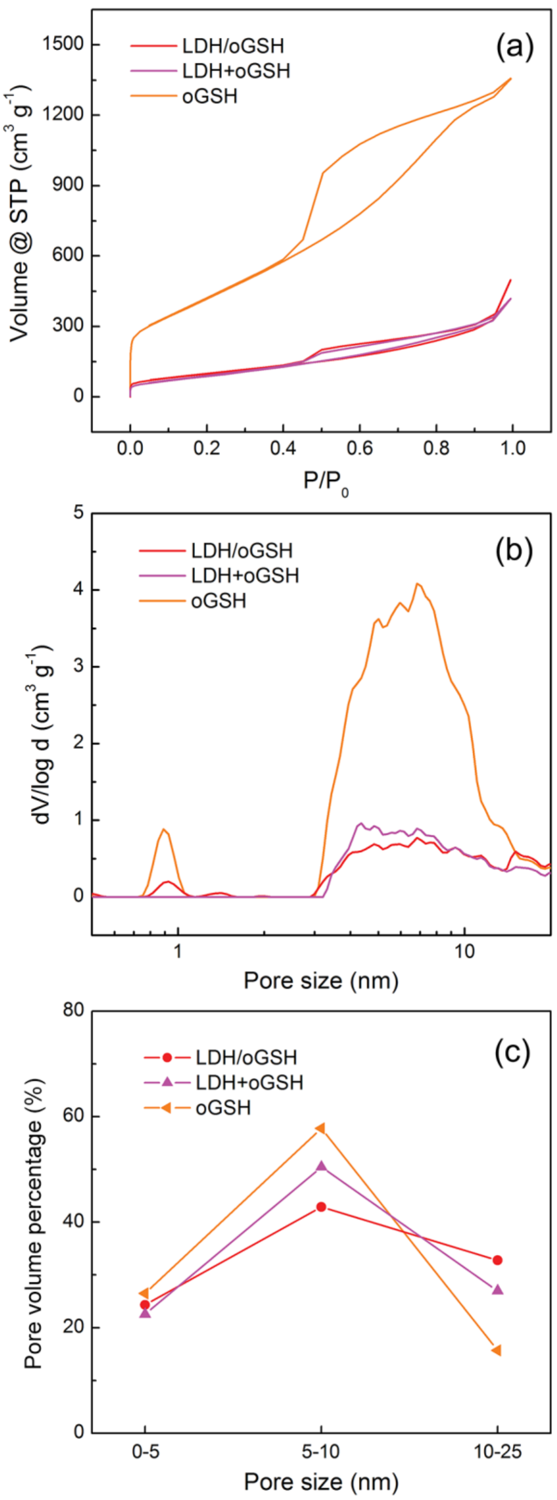

Fig. S4 Pore size analysis results of LDH/oGSH, LDH+oGSH, and oGSH samples. (a) N_2 adsorption-desorption isotherms and (b) the corresponding pore size distributions based on quenched solid density function theory model using the adsorption branch. (c) Cumulative pore size distribution of oGSH comparing with in-situ grown LDHs and mixed LDHs.

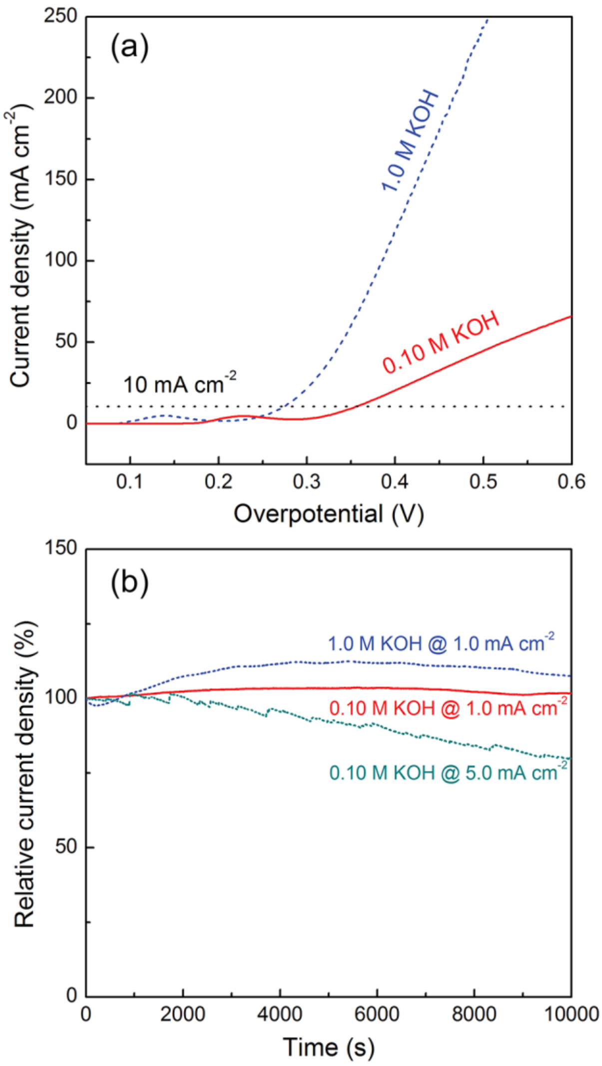

Fig. S5 OER performances of LDH/oGSH in 0.10 and 1.0 M KOH electrolytes. (a) LSV curves and (b) stability test results obtained at different initial current densities.

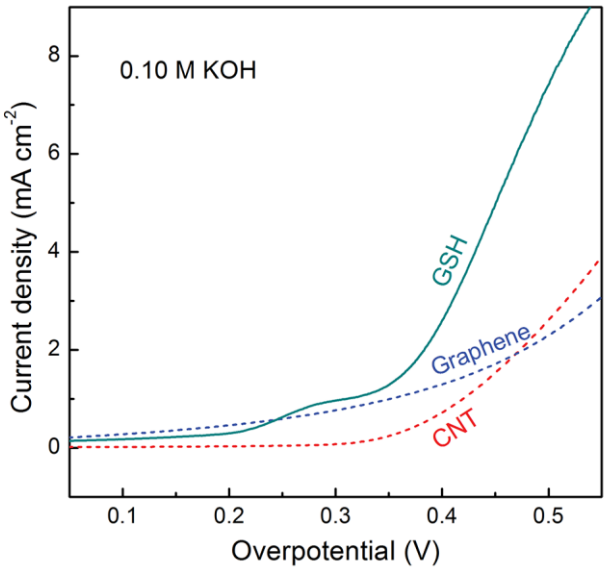

Fig. S6 LSV curves of GSH, as well as graphene and CNT control samples in 0.10 M KOH.

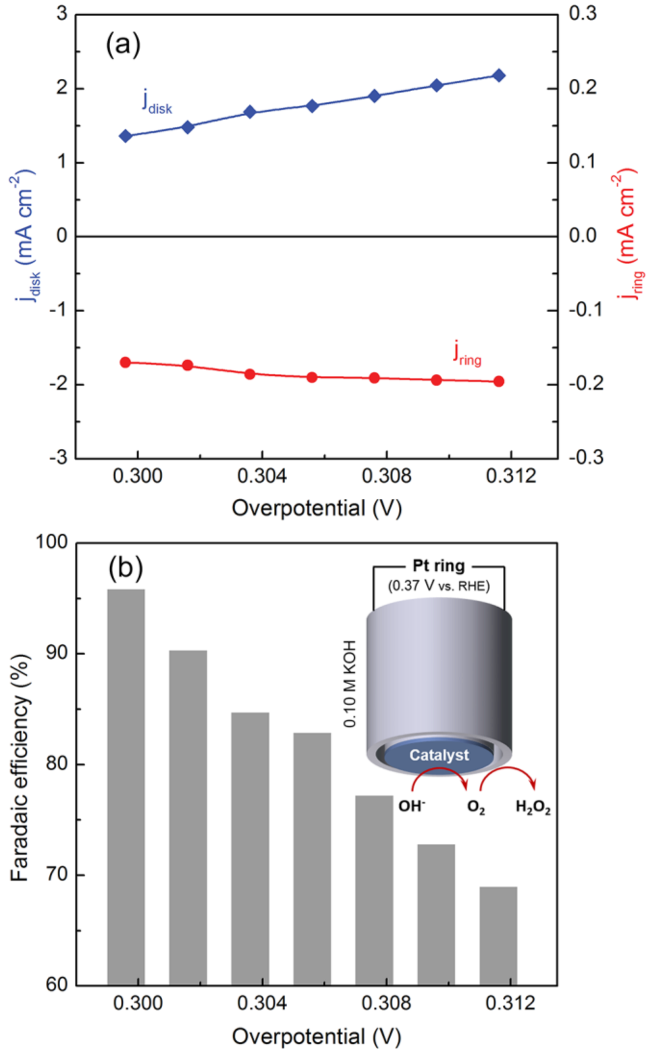

Fig. S7 Faradaic efficiency measurement of LDH/oGSH RRDE at a rotating speed of 1600 rpm in N_2-saturated 0.10 M KOH. (a) The disk and ring current densities and (b) the as-determined Faradaic efficiency plotted against the applied disk overpotential.

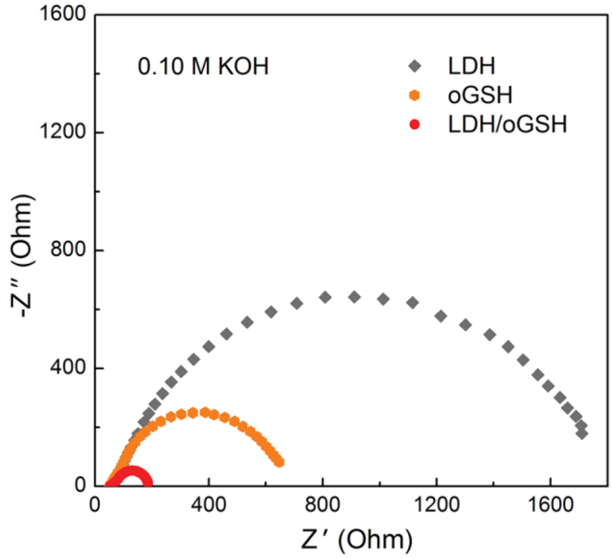

Fig. S8 Nyquist plots of LDH/oGSH and its individual components in 0.10 M KOH, measured at 0.52 V *vs.* SCE over a frequency range from 10 mHz to 10 kHz at the sinusoidal voltage amplitude of 5.0 mV.

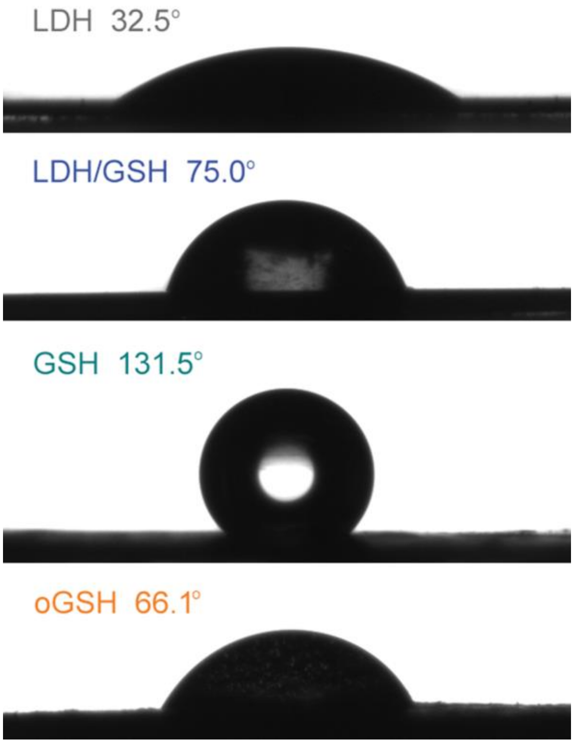

Fig. S9 Contact angles of LDH/GSH and its individual components (*i.e.*, LDH and GSH), as well as oxygen-decorated GSH (*i.e.*, oGSH).

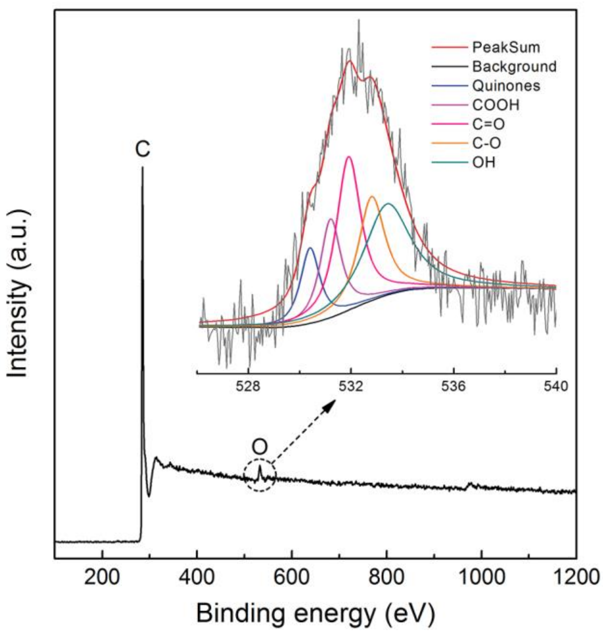

Fig. S10 XPS spectrum of GSH, with the inset presenting the high resolution O 1s spectra.

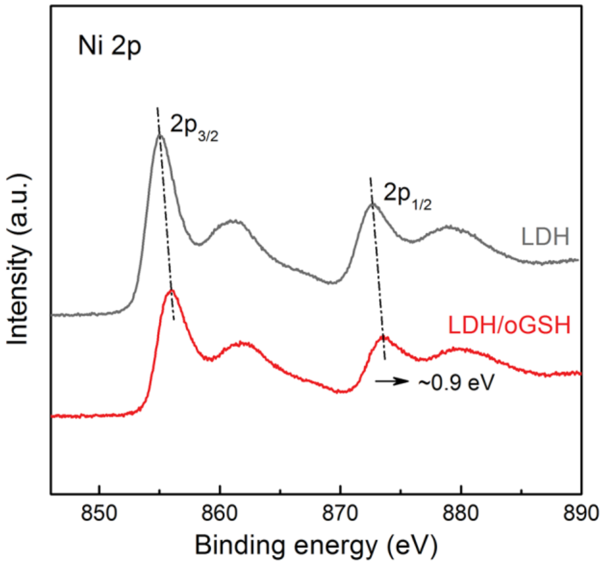

Fig. S11 High resolution Ni 2p spectra of LDH/oGSH and bulk LDH.

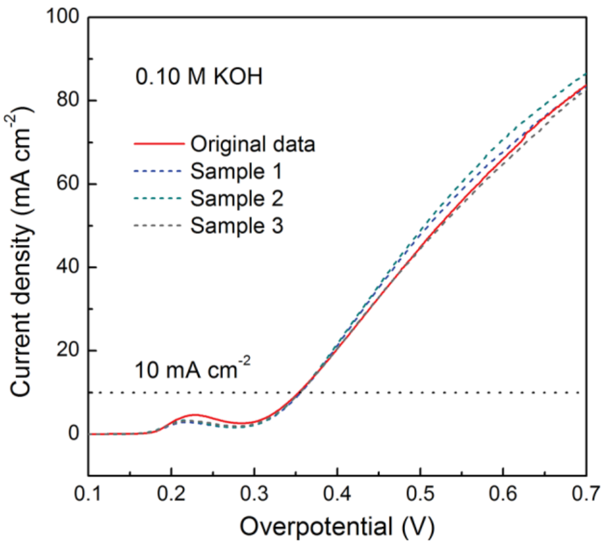

Fig. S12 LSV curves of LDH/oGSH and its three repeated samples in 0.10 M KOH.

2. Supplementary Tables

Table S1 Summary of OER performance of NiFe-based composite electrocatalysts in 0.10 M KOH solution.

Samples	η_{onset} [a] (mV)	η_{10} [b] (mV)	j_{400} [c] (mA cm^{-2})	Tafel slope (mV dec^{-1})	Reference
LDH/oGSH	240	350	21	54	This work
LDH/GSH	255	380	14	58	
LDH+oGSH	260	395	11	61	
LDH	310	530	4	64	
NiFe-LDH/CNT	270	309	-	35	S1
CQD/NiFe-LDH	260	305	-	35	S2
n-NiFe LDH/NGF	250	337	30	45	S3
m-NiFe/CNx	220	360	13	59	S4
3D NiFe-LDH	230	250	-	50	S5
O-NiCoFe-LDH	260	420	9	93	S6
a-$Fe_{40}Ni_{60}O_x$	190	-	6	34 ± 8	S7
Ni-Fe film [40% Fe]	280	420	-	40	S8

[a] OER onset overpotential.

[b] Overpotential required to achieve a current density of 10 mA cm^{-2}.

[c] Current density at an overpotential of 400 mV.

Table S2 Relative atom ratios of oxygen functional groups in graphene/single-walled CNT hybrids before and after oxidation as determined by XPS.

Samples	Oxygen functional groups (at.%)					Sum (at.%)
	Quinones (530.4 eV)	COOH (531.2 eV)	C=O (531.9 eV)	C-O (532.8 eV)	OH (533.4 eV)	
oGSH	0.51	0.88	1.12	0.77	1.35	4.63
GSH	0.20	0.28	0.51	0.38	0.57	1.94

3. Supplementary References

S1 M. Gong, Y. Li, H. Wang, Y. Liang, J. Z. Wu, J. Zhou, J. Wang, T. Regier, F. Wei and H. Dai, *J. Am. Chem. Soc.*, 2013, **135**, 8452.

S2 D. Tang, J. Liu, X. Wu, R. Liu, X. Han, Y. Han, H. Huang, Y. Liu and Z. Kang, *ACS Appl. Mater. Interfaces*, 2014, **6**, 7918.

S3 C. Tang, H. S. Wang, H. F. Wang, Q. Zhang, G. L. Tian, J. Q. Nie and F. Wei, *Adv. Mater.*, 2015, **27**, 4516.

S4 S. Ci, S. Mao, Y. Hou, S. Cui, H. Kim, R. Ren, Z. Wen and J. Chen, *J. Mater. Chem. A*, 2015, **3**, 7986.

S5 Z. Lu, W. Xu, W. Zhu, Q. Yang, X. Lei, J. Liu, Y. Li, X. Sun and X. Duan, *Chem. Commun.*, 2014, **50**, 6479.

S6 L. Qian, Z. Lu, T. Xu, X. Wu, Y. Tian, Y. Li, Z. Huo, X. Sun and X. Duan, *Adv. Energy Mater.*, 2015, **5**, 1500245.

S7 R. D. Smith, M. S. Prévot, R. D. Fagan, S. Trudel and C. P. Berlinguette, *J. Am. Chem. Soc.*, 2013, **135**, 11580.

S8 M. W. Louie and A. T. Bell, *J. Am. Chem. Soc.*, 2013, **135**, 12329.